15. Y. Zhang, Y.-W. Tan, H. L. Stormer, P. Kim, *Nature* **438**, 201–204 (2005).
16. K. S. Novoselov *et al.*, *Nature* **438**, 197–200 (2005).
17. Y. Liu, G. Bian, T. Miller, T.-C. Chiang, *Phys. Rev. Lett.* **107**, 166803 (2011).
18. C. Hwang *et al.*, *Phys. Rev. B* **84**, 125422 (2011).
19. M. Aidelsburger, *et al.*, *Nat. Phys.* **2014**, 10.1038/nphys3171 (2014).
20. G. Jotzu *et al.*, *Nature* **515**, 237–240 (2014).
21. I. B. Spielman, *Annalen der Physik* **525**, 797–807 (2013).
22. M. Aidelsburger *et al.*, *Phys. Rev. Lett.* **107**, 255301 (2011).
23. L. Tarruell, D. Greif, T. Uehlinger, G. Jotzu, T. Esslinger, *Nature* **483**, 302–305 (2012).
24. J. Struck *et al.*, *Nat. Phys.* **9**, 738–743 (2013).
25. M. Aidelsburger *et al.*, *Phys. Rev. Lett.* **111**, 185301 (2013).
26. H. Miyake, G. A. Siviloglou, C. J. Kennedy, W. C. Burton, W. Ketterle, *Phys. Rev. Lett.* **111**, 185302 (2013).
27. N. Goldman, G. Juzeliunas, P. Ohberg, I. B. Spielman, *Rep. Prog. Phys.* **77**, 126401 (2014).
28. M. Ben Dahan, E. Peik, J. Reichel, Y. Castin, C. Salomon, *Phys. Rev. Lett.* **76**, 4508–4511 (1996).
29. M. Greiner, I. Bloch, O. Mandel, T. W. Hänsch, T. Esslinger, *Phys. Rev. Lett.* **87**, 160405 (2001).
30. S.-L. Zhu, B. Wang, L.-M. Duan, *Phys. Rev. Lett.* **98**, 260402 (2007).
31. P. Dietl, F. Piéchon, G. Montambaux, *Phys. Rev. Lett.* **100**, 236405 (2008).
32. L. Fallani *et al.*, *Phys. Rev. Lett.* **93**, 140406 (2004).
33. C. D'Errico *et al.*, *New J. Phys.* **9**, 223 (2007).
34. I. Carusotto, C. Ciuti, *Rev. Mod. Phys.* **85**, 299–366 (2013).
35. F. Grusdt, D. Abanin, E. Demler, *Phys. Rev. A* **89**, 043621 (2014).
36. P. Zanardi, M. Rasetti, *Phys. Lett. A* **264**, 94–99 (1999).
37. S. A. Parameswaran, R. Roy, S. L. Sondhi, *C. R. Phys.* **14**, 816–839 (2013).
38. A. K. Tuchman, M. A. Kasevich, *Phys. Rev. Lett.* **103**, 130403 (2009).

ACKNOWLEDGMENTS

We acknowledge technical assistance by M. Boll, H. Lüschen, and J. Bernardoff during the setup of the experiment and thank E. Demler, D. Abanin, and X.-L. Qi for helpful discussions. We acknowledge financial support by the Deutsche Forschungsgemeinschaft (FOR801), the European Commission (UQUAM), the U.S. Defense Advanced Research Projects Agency Optical Lattice Emulator program, the Nanosystems Initiative Munich, and the Alfred P. Sloan Foundation.

SUPPLEMENTARY MATERIALS

www.sciencemag.org/content/347/6219/288/suppl/DC1
Supplementary Text
Figs. S1 to S3
References (*39*–*49*)

22 July 2014; accepted 5 December 2014
Published online 18 December 2014;
10.1126/science.1259052

INTERFACIAL SOLVENTS

Universal solvent restructuring induced by colloidal nanoparticles

Mirijam Zobel,[1]* Reinhard B. Neder,[1] Simon A. J. Kimber[2]*

Colloidal nanoparticles, used for applications from catalysis and energy applications to cosmetics, are typically embedded in matrixes or dispersed in solutions. The entire particle surface, which is where reactions are expected to occur, is thus exposed. Here, we show with x-ray pair distribution function analysis that polar and nonpolar solvents universally restructure around nanoparticles. Layers of enhanced order exist with a thickness influenced by the molecule size and up to 2 nanometers beyond the nanoparticle surface. These results show that the enhanced reactivity of solvated nanoparticles includes a contribution from a solvation shell of the size of the particle itself.

Bulk liquids have long been known to show short-range order. The original method of choice was x-ray scattering, which was used by Zachariasen in 1935 to study the short-range order between solvent molecules (*1*). Alcohol molecules were shown to form a hydrogen-bonded network within the bulk solvent (*2*–*4*), and short alkanes were found to align in parallel within domains of ~2 nm (*5*). More recently, the influence of hard planar walls on bulk liquids has been investigated (*6*–*8*). Together with force measurements (*7*, *8*), x-ray scattering confirmed that an exponentially decaying oscillatory density profile is established near the interface (*9*). With the advent of synchrotron radiation sources, Magnussen *et al.* showed by use of x-ray reflectivity that even liquid mercury orders at a flat solid interface in exactly the same way (*9*). More recent examples of such ordering phenomena at interfaces include the restructuring of nonpolar n-hexane (*10*), the assembly of fluorinated ionic liquids at sapphire surfaces (*11*), and the exponentially decaying surface segregation profiles in Cu_3Au alloy interfaces (*12*). These restructuring phenomena—in particular, the interlayer spacings and decay lengths—are closely related to the local ordering in the bulk liquid (*9*, *12*).

Although the reorganization of solvent molecules around isolated cations in solution has also been explored (*13*, *14*), comparable studies on solvated nanoparticles (NPs) are rare, in particular for nonaqueous solvent (*15*–*17*). Solvent molecules are expected and have theoretically been modeled (*15*, *16*) to rearrange at the liquid-NP interface, although no definitive experimental proof exists so far. For bulk planar surfaces (*6*–*8*) and ions (*13*, *14*), such enhanced order is well understood. Here, we report a synchrotron x-ray scattering study of a variety of as-synthesized and commercial NPs in polar and nonpolar solvents. We show enhanced ordering of solvent molecules at the NP surface that extends several layers into the bulk liquid. This effect is largely independent of the capping agent, solvent polarity, and particle size.

We systematically redispersed different types of metal and metal oxide NPs in polar and nonpolar organic solvents (*18*). We studied the influence of the solvent molecule size within the series of primary alcohols (methanol, ethanol, and 1-propanol) and the effect on nonpolar solvents with hexane. Fourier transformation of high-energy x-ray scattering patterns yielded the pair distribution functions (PDFs), histograms of all interatomic distances within a sample. Data treatment includes the subtraction of diffraction data of the respective pure solvent so that the signal from the bulk solvent is subtracted before the Fourier transformation. The

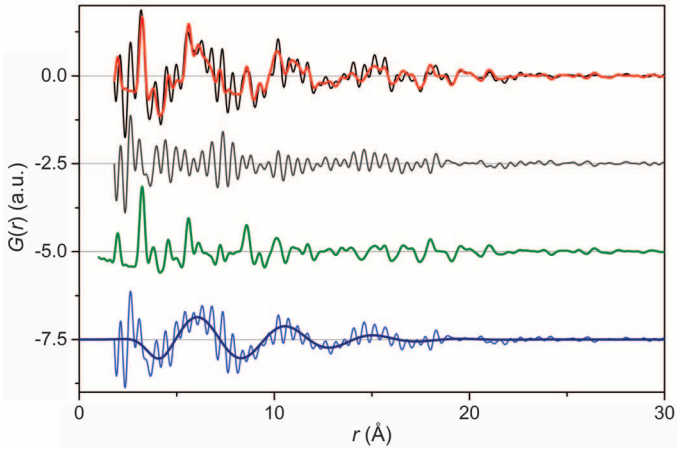

Fig. 1. Fit to the PDF of redispersed ZnO NPs with citrate ligands in propanol. Experimental d-PDF of ZnO NPs (black) and their fit (red), showing the overall difference of the fit (gray), the contribution of the NP (green), and the contribution and fit of the restructured solvent (blue) in offset for means of clarity. The contribution of the restructured solvent (blue) is the dd-PDF of the experimental, background-corrected d-PDF (black) and the NP (green).

[1]Department of Physics, Lehrstuhl für Kristallographie und Strukturphysik, Friedrich-Alexander University Erlangen-Nürnberg, Staudtstrasse 3, 91058 Erlangen, Germany. [2]European Synchrotron Radiation Facility, 71 Avenue des Martyrs, 38000 Grenoble, France.
***Corresponding author. E-mail: mirijam.zobel@fau.de (M.Z.); kimber@esrf.fr (S.A.J.K.)**

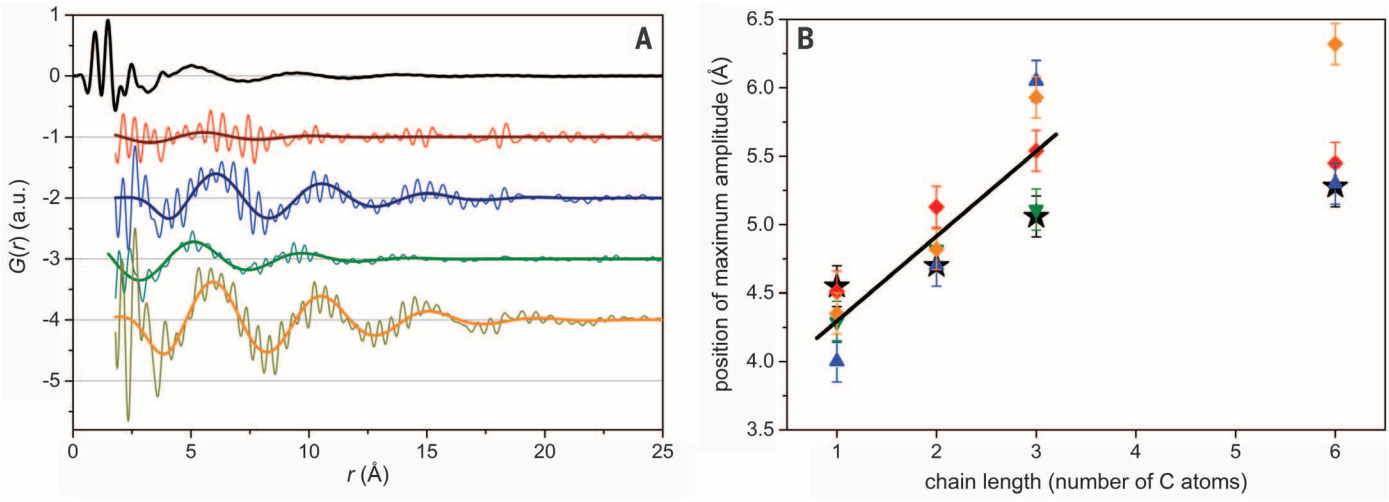

Fig. 2. Comparison of short-range order in restructured and bulk solvents. (**A**) PDF of pure bulk propanol (black) and dd-PDFs of restructured propanol around ZnO NPs with ligand acetate (red), citrate (blue), dmlt (green), and pent (yellow). The amplitudes of the dd-PDFs are scaled with respect to the contribution of ZnO NPs to the data. (**B**) Maxima positions of dd-PDFs of the redispersed ZnO NPs in all solvents plotted over the chain length of the solvent molecules. The positions follow the trend of the pure solvents (black stars), yet the dd-PDF positions are distinctly offset with respect to the error bars that resulted from least-squares fits.

resulting difference PDF (d-PDF) should only contain peaks from intraparticular distances within the NPs and hence be identical to the PDF of a NP powder sample. We observed, however, a distinct, exponentially damped sinusoidal oscillation, which vanished in dry samples (Fig. 1; further examples are shown in figs. S7 and S8) (*18*). A least-squares fit (red) of the linear combination of the respective NP powder (green) and an exponentially decaying sinusoidal oscillation (blue) describes all data sets (black) adequately (*18*) and gives access to four parameters that describe the restructuring: (i) the amplitude, (ii) the position of the first maximum of the oscillation, (iii) the wavelength, and (iv) the modulation depth [calculations are provided in (*18*)]. The amplitude contains information about how many solvent molecules restructure, and the modulation depth describes how far this enhanced ordering extents into the bulk liquid. The position and wavelength describe the arrangement and layer spacing of the molecules.

The PDF of bulk propanol is shown in Fig. 2A together with the double-difference PDFs (dd-PDFs) of the restructured solvent and their fits for four different ZnO NPs in propanol. Here, the dd-PDF is the difference between the d-PDF of the redispersed sample and the PDF of the NP powder. The resulting dd-PDFs differ from the PDF of the pure solvent in that they exhibit a distinctively larger modulation depth. In contrast to bulk propanol, the dd-PDFs do not show sharp intramolecular distances of the propanol molecules in the range 0 to 3 Å because they are entirely corrected for in the background subtraction. The restructuring does not change the internal molecular structure but only changes the relative orientation between different solvent molecules. Thus, the enhanced short-range order around the NPs becomes visible as the oscillation in the dd-PDF. We observed the same kind of restructuring for a wide range of metal oxide and metal NPs (figs. S5 and S6) (*18*).

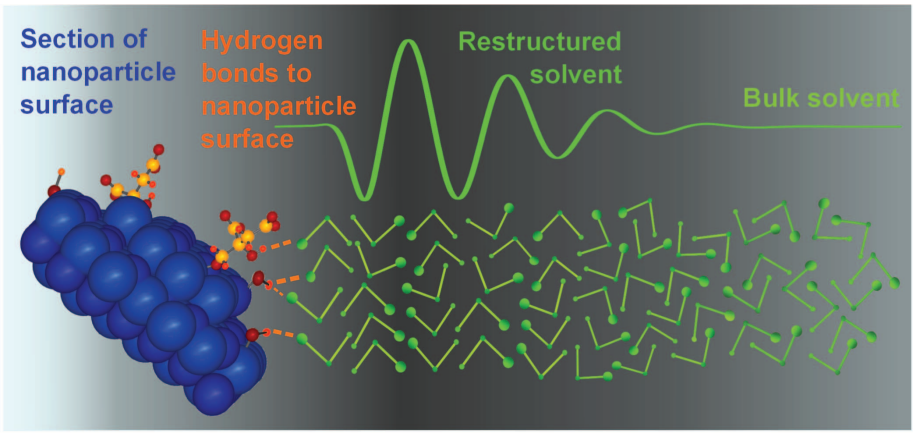

Fig. 3. Enhanced short-range order of solvent molecules at ZnO NP surfaces. The ethanol molecules (hydrogen atoms omitted) form hydrogen bonds with surface hydroxyl groups and citrate molecules. The surface coverage of these groups is reduced for means of clarity. The enhanced short-range order extends a few molecular layers into the bulk liquid before bulk properties are recovered. In bulk ethanol, molecules do not arrange in pairs, but form winding-chains or hexamers (*2*–*4*), and the enhanced short-range order around the NPs is not as crystalline as suggested in the scheme, which serves as simplified illustrative representation.

In essence, the PDF represents the distribution of all interatomic distances *r*. Because we work in a highly diluted system, we can expect that the structure of the bulk solvent does not change. Likewise, the contribution of the NPs to the PDF does not differ from that of the PDF of the pure NP. Because all changes to the experimental dd-PDF occur upon redispersing the NP in the pure solvent, these changes must be induced by the NP surfaces (*18*). Thus, our dd-PDFs represent a change of the short-range order within the solvent near the NP surface. With increasing distance, the signal in the dd-PDF exponentially decays. The orientational averaging intrinsic to the PDF technique prevents us from determining the direction of rearrangement; however, the signal bears a striking similarity to those seen by using specular x-ray surface scattering, which probes only the direction normal to the interface.

A comparison of the maximum position, wavelength, and modulation depth of the oscillation for our ZnO NPs is shown in Fig. 2B and fig. S5. A linear trend in the position of the maximum amplitude is found with alcohol chain length. Furthermore, this trend occurs for four different capping agents, showing that surface composition plays a minor role. A larger spread in these

parameters is found for other types of NPs (Ag, ZrO_2, TiO_2, and In_2O_3) (fig. S6). These results show that to first approximation, and in agreement with MD simulations (*15*), the microscopic details of the NP surface only weakly influence the solvent restructuring. However, it is possible that the spread of data points in Fig. 2B, which increases for increasing alkyl chain length, indicates an additional role for particle shape, surface restructuring, or differences in capping agent. Our model of restructuring for ethanol at the surface of a ZnO NP decorated with citrate and hydroxyl groups of capping ligands is illustrated in Fig. 3. The surface coverage of NPs with organic ligand molecules is sufficient to prevent agglomeration but in fact is unexpectedly small according to neutron PDF data (*19*) and nuclear magnetic resonance (NMR) studies (*20*). MD simulations (*15*, *21*, *22*), in agreement with experimental evidence from NMR (*20*), suggest that the vast majority of ZnO surface sites are terminated by hydroxyl groups. These could form a hydrogen-bonded network with adjacent solvent molecules.

Because of the shift in the oscillation with the solvent size, we conclude that the alcohol molecules tend to align perpendicular to the NP surface. Their hydroxyl groups form hydrogen bonds with the ligand molecules and hydroxyl groups. The alkyl chains of the solvent point away from the NP surface. The next- and second-next–neighboring molecules align so that hydrogen bonds can be formed within the solvent, which results in alternating layers of methyl groups and hydroxyl groups, building layers of decreased and enhanced electron density, as depicted in Fig. 3. Adjacent molecules within such a layer would orient in parallel, as observed for liquid films (*23*). The extent of restructuring depends on the solvent size and packing ability. Here, the packing ability is comparable for our alcohols because the hydroxyl group is always in a terminal position and the alkane chain is not branched. A second-harmonic generation (SHG) study on the interaction of organic solvent and solute molecules with hydroxylated silica surfaces supports our hydrogen bonding model (*24*). This study also showed that nonpolar solvents rearrange at hydroxylated surfaces, which supports our observation that the nonpolar n-hexane restructures at the NP surfaces. However, SHG is only sensitive to broken symmetry at interfaces, whereas it cannot provide information on the decay of the restructuring into the bulk liquid, as evidenced by our dd-PDFs.

REFERENCES AND NOTES

1. W. H. Zachariasen, *J. Chem. Phys.* **3**, 158–161 (1935).
2. D. L. Wertz, R. K. Kruh, *J. Chem. Phys.* **47**, 388–390 (1967).
3. C. J. Benmore, Y. L. Loh, *J. Chem. Phys.* **112**, 5877–5883 (2000).
4. A. Vrhovšek, O. Gereben, A. Jamnik, L. Pusztai, *J. Phys. Chem. B* **115**, 13473–13488 (2011).
5. G. W. Longman, G. D. Wignall, R. P. Sheldon, *Polymer (Guildf.)* **20**, 1063–1069 (1979).
6. B. Götzelmann, A. Haase, S. Dietrich, *Phys. Rev. E Stat. Phys. Plasmas Fluids Relat. Interdiscip. Topics* **53**, 3456–3467 (1996).
7. J. Israelachvili, *Acc. Chem. Res.* **20**, 415–421 (1987).
8. I. K. Snook, W. van Megen, *J. Chem. Phys.* **72**, 2907 (1980).
9. O. M. Magnussen *et al.*, *Phys. Rev. Lett.* **74**, 4444–4447 (1995).
10. A. Doerr, M. Tolan, T. Seydel, W. Press, *Physica B* **248**, 263–268 (1998).
11. M. Mezger *et al.*, *Science* **322**, 424–428 (2008).
12. H. Reichert, P. J. Eng, H. Dosch, I. K. Robinson, *Phys. Rev. Lett.* **74**, 2006–2009 (1995).
13. D. T. Bowron, S. Díaz-Moreno, *J. Phys. Chem. B* **113**, 11858–11864 (2009).
14. R. Mancinelli, A. Botti, F. Bruni, M. A. Ricci, A. K. Soper, *Phys. Chem. Chem. Phys.* **9**, 2959–2967 (2007).
15. D. Spagnoli, J. P. Allen, S. C. Parker, *Langmuir* **27**, 1821–1829 (2011).
16. B. H. G. Hertz, I. An, *Angew. Chem. Int. Ed. Engl.* **9**, 124–138 (1970).
17. R. S. Cataliotti, F. Aliotta, R. Ponterio, *Phys. Chem. Chem. Phys.* **11**, 11258–11263 (2009).
18. Materials and methods are available as supplementary materials on *Science* Online.
19. K. Page, T. C. Hood, T. Proffen, R. B. Neder, *J. Appl. Cryst.* **44**, 327–336 (2011).
20. C. N. Valdez, A. M. Schimpf, D. R. Gamelin, J. M. Mayer, *ACS Nano* **8**, 9463–9470 (2014).
21. A. Kawska, P. Duchstein, O. Hochrein, D. Zahn, *Nano Lett.* **8**, 2336–2340 (2008).
22. D. Raymand, A. C. T. Duin, W. A. Goddard III, K. Hermansson, D. Spångberg, *J. Phys. Chem. C* **115**, 8573–8579 (2011).
23. H. K. Christenson, D. W. R. Gruen, R. G. Horn, J. N. Israelachvili, *J. Chem. Phys.* **87**, 1834 (1987).
24. X. Zhang, M. M. Cunningham, R. A. Walker, *J. Phys. Chem. B* **107**, 3183–3195 (2003).

ACKNOWLEDGMENTS

We acknowledge the Bundesministerium für Bildung, Wissenschaft, Forschung und Technologie under grant 05K10WEB and a scholarship of the Friedrich-Alexander-University Erlangen-Nürnberg for financial support. Beam time at the European Synchrotron Radiation Facility and Argonne National Laboratory is gratefully acknowledged. We thank J. Hudspeth from beamline ID-15-B, European Synchrotron Radiation Facility, as well as K. Chapman and K. Beyer from beamline 11-ID-B, and Advanced Proton Source for support during our beamtime. We acknowledge A. Magerl and H. Reichert for discussions. All experimental raw data are stored at the European Synchrotron Radiation Facility. For access, please contact S.A.J.K. (kimber@esrf.fr).

SUPPLEMENTARY MATERIALS

www.sciencemag.org/content/347/6219/292/suppl/DC1
Materials and Methods
Supplementary Text
Figs. S1 to S11
Table S1
References (*25*–*33*)

18 September 2014; accepted 26 November 2014
10.1126/science.1261412

PHYSICS

Observation of Fermi arc surface states in a topological metal

Su-Yang Xu,[1,2]* Chang Liu,[1]* Satya K. Kushwaha,[3] Raman Sankar,[4] Jason W. Krizan,[3] Ilya Belopolski,[1] Madhab Neupane,[1] Guang Bian,[1] Nasser Alidoust,[1] Tay-Rong Chang,[5] Horng-Tay Jeng,[5,6] Cheng-Yi Huang,[7] Wei-Feng Tsai,[7] Hsin Lin,[8] Pavel P. Shibayev,[1] Fang-Cheng Chou,[4,9] Robert J. Cava,[3] M. Zahid Hasan[1,2]†

The topology of the electronic structure of a crystal is manifested in its surface states. Recently, a distinct topological state has been proposed in metals or semimetals whose spin-orbit band structure features three-dimensional Dirac quasiparticles. We used angle-resolved photoemission spectroscopy to experimentally observe a pair of spin-polarized Fermi arc surface states on the surface of the Dirac semimetal Na_3Bi at its native chemical potential. Our systematic results collectively identify a topological phase in a gapless material. The observed Fermi arc surface states open research frontiers in fundamental physics and possibly in spintronics.

The realization of topological states of matter beyond topological insulators has become an important goal in condensed-matter and materials physics (*1*–*15*). In the topological insulators $Bi_{1-x}Sb_x$ and Bi_2Se_3 or topological crystalline insulators such as $Pb_{1-x}Sn_xTe(Se)$, the bulk has a full insulating energy gap, whereas the surface possesses an odd or even number of spin-polarized surface or edge states (*3*, *14*–*18*). These are symmetry-protected topological states (*19*). Very recently, the possibility of realizing new topological states in materials beyond insulators, such as metals or semimetals, has attracted much attention (*1*–*13*). Semimetals are materials whose bulk conduction and valence bands have small but finite overlap; the lack of a full band-gap implies that any topological states that might exist in a semimetal should be distinct from the topological states studied in insulating materials. Theory has proposed two kinds of topological semimetals: the topological Dirac and Weyl semimetals (*2*, *7*–*12*). Their low-energy bulk excitations are described by the Dirac and Weyl equations, respectively. For both types, the bulk conduction and valence bands are predicted to touch at multiple discrete points in the bulk Brillouin zone

[1]Joseph Henry Laboratory, Department of Physics, Princeton University, Princeton, NJ 08544, USA. [2]Princeton Center for Complex Materials, Princeton Institute for Science and Technology of Materials, Princeton University, Princeton, NJ 08544, USA. [3]Department of Chemistry, Princeton University, Princeton, NJ 08544, USA. [4]Center for Condensed Matter Sciences, National Taiwan University, Taipei 10617, Taiwan. [5]Department of Physics, National Tsing Hua University, Hsinchu 30013, Taiwan. [6]Institute of Physics, Academia Sinica, Taipei 11529, Taiwan. [7]Department of Physics, National Sun Yat-Sen University, Kaohsiung 804, Taiwan. [8]Graphene Research Centre and Department of Physics, National University of Singapore 117542. [9]National Synchrotron Radiation Research Center, Taiwan.
*These authors contributed equally to this work. †Corresponding author. E-mail: mzhasan@princeton.edu

Universal solvent restructuring induced by colloidal nanoparticles

Mirijam Zobel, Reinhard B. Neder and Simon A. J. Kimber (January 15, 2015)

Science **347** (6219), 292-294. [doi: 10.1126/science.1261412]

Editor's Summary

Structured solvents near nanoparticles

The physical properties and reactivity of nanoparticles in solution depend not only on their surface termination but also on changes in solvent ordering caused by the presence of the interface created by the nanoparticle. Zobel *et al.* used x-ray scattering to study solvent ordering for a variety of metal and metal-oxide nanoparticles in a variety of polar solvents (alcohols) and a nonpolar solvent (n-hexane). They observed layers of enhanced ordering near the nanoparticle surface relative to the bulk solvent. These trends were largely independent of surface chemistry, such as changing the surface groups from hydroxyls to carboxylates.

Science, this issue p. 292